ADVANCED MATERIALS
www.advmat.de

A Rotating Cathode with Periodical Changes in Electrolyte Layer Thickness for High-Rate Li–O_2 Batteries

Yu-Long Liang, Yue Yu, Zi-Wei Li, Dong-Yue Yang, Tong Liu, Jun-Min Yan, Gang Huang, and Xinbo Zhang**

Li–O_2 batteries (LOBs) possess the highest theoretical gravimetric energy density among all types of secondary batteries, but they are still far from practical applications. The poor rate performance resulting from the slow mass transfer is one of the primary obstacles in LOBs. To solve this issue, a rotating cathode with periodic changes in the electrolyte layer thickness is designed, decoupling the maximum transfer rate of Li^+ and O_2. During rotation, the thinner electrolyte layer on the cathode facilitates the O_2 transfer, and the thicker electrolyte layer enhances the Li^+ transfer. As a result, the rotating cathode enables the LOBs to undergo 58 cycles at 2.5 mA cm^{-2} and discharge stably even at a high current density of 7.5 mA cm^{-2}. Besides, it also makes the batteries exhibit a large discharge capacity of 6.8 mAh cm^{-2}, and the capacity decay is much slower with increasing current density. Notably, this rotating electrode holds great promise for utilization in other electrochemical cells involving gas-liquid-solid triple-phase interfaces, suggesting a viable approach to enhance the mass transfer in such systems.

1. Introduction

Li–O_2 batteries (LOBs) have garnered significant attention due to their highest theoretical energy density (≈5200 Wh kg^{-1} based on Li_2O and 3500 Wh kg^{-1} based on Li_2O_2) among all the candidates of battery systems.[1] However, they have long been plagued by several issues, including but not limited to poor rate performance, large voltage hysteresis, and severe parasitic reactions.[2] The poor rate performance of LOBs hinders their practical applications.[3] For instance, the full discharge of a punch LOB could take 33 days to achieve passable energy density, which makes it difficult to meet consumer demand.[4] Therefore, improving the rate performance is urgent and important for the practical application of LOBs. It is widely accepted that the poor rate performance of LOBs is primarily attributed to the sluggish mass transfer, rather than the kinetics of electrode reactions.[1b,5] For LOBs, the mass transfer includes the transfer of Li^+ and O_2. Some researchers believe that the choice of electrolyte solvent has a major influence on the O_2 transfer.[5a] However, until now, researchers have not discovered an electrolyte that is completely stable against the Li anode and reactive oxygen species,[6] which makes it challenging to solely improve the O_2 transfer through electrolyte modifications, as do the redox mediators (RMs). Therefore, finding ways to accelerate the O_2 transfer within the existing electrolyte systems is of great importance. Another often adopted approach involves designing the customized cathode structure. It has been demonstrated that the cathode with hierarchical pores could boost the battery performance to some extent.[7] Specifically, macropores (width > 50 nm) are thought to offer sufficient spaces for O_2 diffusion and discharge product storage.[8] However, the available studies overlook the wetting behavior between the electrolyte and cathode. O_2 cannot easily flow through the existing pores if the pores within the cathode are fully immersed in the electrolyte. Some researchers have recognized this issue and they attempt to improve the O_2 transfer by adjusting the hydrophilicity between the electrolyte and cathode.[9] However, this method still does not work well due to the accumulation of discharge products.

The transfer of Li^+ is also a crucial part of mass transfer in LOBs but has been overlooked by most researchers. As we know, the concentration of lithium salts in electrolytes is typically high enough, and the mobility of Li^+ in the electrolyte of LOBs is comparable to that in Li-ion batteries (LIBs), which have achieved quite good rate performance. However, due to the requirement of three-phase reaction interfaces in LOBs, the abundant O_2 transmission channels constructed in the cathode will make Li^+ transfer more challenging than LIBs. In addition, the transfer distance of Li^+ in LOBs is typically longer than that in LIBs. A typical

Y.-L. Liang, Z.-W. Li, J.-M. Yan
Key Laboratory of Automobile Materials
Ministry of Education
Department of Materials Science and Engineering
Jilin University
Changchun 130022, China

Y.-L. Liang, Z.-W. Li, D.-Y. Yang, T. Liu, G. Huang, X. Zhang
State Key Laboratory of Rare Earth Resource Utilization
Changchun Institute of Applied Chemistry
Chinese Academy of Sciences
Changchun 130022, China
E-mail: ghuang@ciac.ac.cn; xbzhang@ciac.ac.cn

Y. Yu
Department of Chemistry and Waterloo Institute for Nanotechnology
University of Waterloo
Waterloo, ON N2L 3G1, Canada

The ORCID identification number(s) for the author(s) of this article can be found under https://doi.org/10.1002/adma.202403230

DOI: 10.1002/adma.202403230

thickness of cathode in LOBs is around 200 µm, which is much thicker than the high-rate LIBs (cathode thickness: 50 µm), and the thicker cathode would result in inferior power performance due to the restricted Li^+ transfer rate.[10]

A factor that significantly affects the transfer of both Li^+ and O_2 is the thickness of the electrolyte layer on the cathode side.[11] On one hand, a thin electrolyte layer would hinder the transfer of Li^+. On the other hand, it could allow O_2 to pass through the liquid phase to the electrode surface quickly.[12] Therefore, there exists an optimal thickness to maximize the mass transfer efficiency.[11a] The optimal thickness of the electrolyte layer varies for each battery system, and its existence could also limit the maximum oxygen reduction reaction (ORR) rate of LOBs. To this end, we have designed a homemade device with a rotating cathode for high-rate LOBs. When rotating the cathode, the thickness of the electrolyte layer on the electrode surface periodically changes. As the electrolyte layer becomes thinner, the oxygen can rapidly reach the electrode surface from the gas phase. Subsequently, as the cathode rotates back into the bulk electrolyte, the transfer rate of Li^+ returns to its maximum value. As a result, the battery with the rotating cathode exhibits 58 cycles at 2.5 mA cm^{-2} and could discharge stably at a high current density of 7.5 mA cm^{-2}, which is much better than the reported conventional LOBs. Besides, a large discharge capacity of 6.8 mAh cm^{-2} can be achieved at 3 mA cm^{-2}.

2. Result and Discussion

2.1. Process of O_2 Transfer and the Limitation of Rate Performance

The influence of the electrolyte thickness at the cathode side on the rate performance is investigated via a homemade cell shown in **Figure 1a** and Figure S1, Supporting Information. In this cell, carbon paper and Li foil are employed as the cathode and anode, respectively. They are connected to the circuit through two pieces of copper foil current collectors. To ensure good contact between the electrodes and current collectors, a slot is pressed on both the cathode and anode. The accurate bottom area of the slot allows us to control the thickness of the electrolyte by adjusting the amount of electrolyte. With this kind of design, each milliliter of electrolyte raises the electrolyte level by 460 µm. Figure 1b illustrates the process of O_2 transfer that consists of three different stages: the transport from the gas phase to the interface, the passage through the gas-electrolyte interface, and the migration within the liquid phase towards the electrode surface. The O_2 could move rapidly in the gas phase, including both convection and diffusion. In terms of diffusion alone, the diffusion rate of O_2 in the gas phase is four orders of magnitude higher than that in the liquid phase,[6] not to mention that the convection is even faster than diffusion. Therefore, the transfer of O_2 in the gas phase does not act as the rate-determining step in the overall O_2 transfer process.

To explore the impact of the latter two stages on the overall O_2 transfer, a linear sweep voltammetry (LSV) test of LOBs with different amounts of electrolyte was carried out (Figure 1c). When the electrolyte layer is relatively thin (≈2–6 mL, ≈0.92–2.76 mm), the current rises with the increase in electrolyte dosage. It requires 3 mL of electrolyte to completely submerge the cathode, and the increase in current less than this amount can be mainly attributed to the increased electrochemically active surface area. The current increase brought by additional electrolyte dosage comes from the increase in Li^+ transfer rate, considering that thickening the electrolyte is detrimental to the O_2 transfer. To prove this point, an LSV test of the battery with 4 mL electrolyte under different O_2 pressures was conducted (Figure S2, Supporting Information). It is clear that the current experiences no obvious change with different O_2 pressures, indicating that the rate performance of batteries with thin electrolyte layers is limited by the transfer of Li^+. However, as the amount of electrolyte reaches ≈7 mL, the transfer of O_2 turns to be the rate-determining step (Figure 1c). Continuously adding electrolyte to around 8 mL, a noticeable decrease in current is observed in the high overpotential region. Since adding 1 mL of additional electrolyte only increases its thickness without affecting the gas-electrolyte interface, it can be concluded that the diffusion of O_2 in the electrolyte has a greater impact on the overall O_2 transfer rate. Besides, an important difference between the O_2 and Li^+ is that the O_2 is electrically neutral while Li^+ is positively charged. This means that the transfer of Li^+ will continue to increase with increasing overpotential, but O_2 does not. Therefore, when the transfer of Li^+ is the rate-determining step, the current will continue to increase with the overpotential, while the current determined by O_2 tends to be a constant value.

It is essential to emphasize that the designed homemade setup amplifies the impact of Li^+ transfer compared to the conventional coin-type LOBs because of the incremental distance between the cathode and anode. The significance of this experiment lies in the analysis of the three stages of O_2 transfer and their individual effects on the overall rate of O_2 transfer. It also reveals that there is indeed an optimal electrolyte thickness for each battery system to achieve the best rate capability.

2.2. Design and Manufacture of the Battery with a Rotating Cathode

To overcome the limitation of mass transfer in LOBs, a rotating battery has been designed, and its interior structure is shown in **Figure 2a,b**, respectively. Part 1 serves as the battery holder to support the rotating cathode and hold the electrolyte, which is made of aluminum with surface oxidation treatment. As lithium metal has a lower density than the electrolyte, two spacers (part 2) were designed to ensure close contact between the lithium metal and the current collector. Part 3 is a U-shaped metal sheet, serving as the current collector of the anode, and a piece of lithium will be tightly pressed onto it before cell assembly. Both parts 2 and 3 are made of copper to ensure the electrochemical stability. Part 4 is the rotating electrode equipped with two bearings on its axis that guarantee stable rotation and minimize friction. Part 4 is made of stainless steel and maintains a polished surface throughout the entire experiment. A piece of carbon cloth is attached to the rotating electrode to act as the cathode. The rotation speed of the cathode could be continuously adjusted from several rpm to thousands of rpm by a motor and a conductive slip ring (Figure S3, Supporting Information). The conductive slip ring guarantees consistent contact between the electrode and the testing equipment. The distance between the cathode and

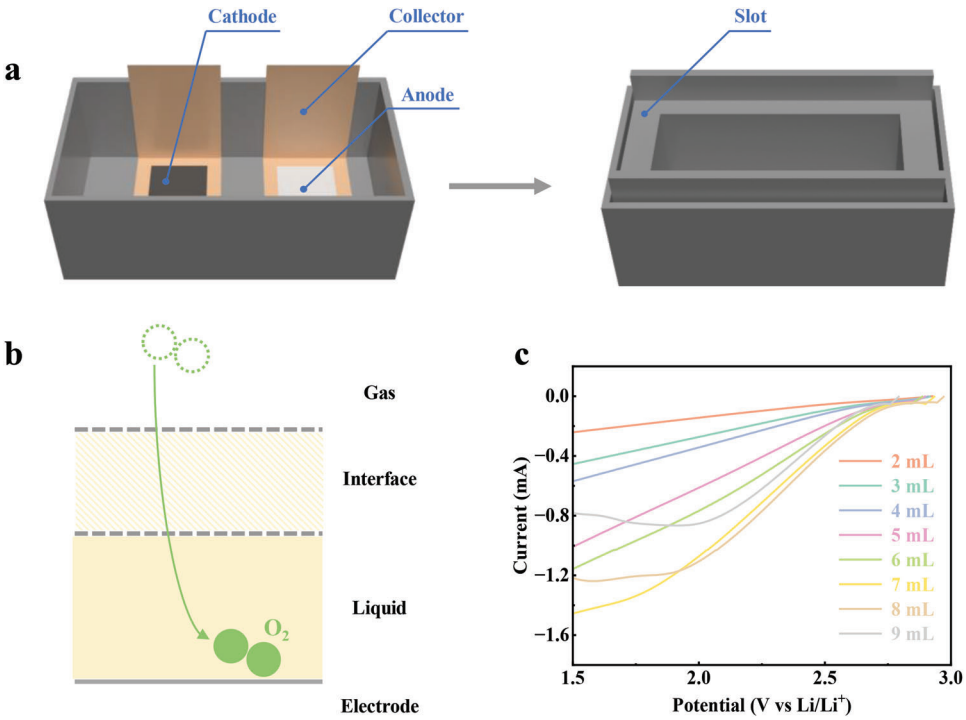

Figure 1. a) Schematic diagram of the homemade LOB. b) Illustration of the O_2 transfer process. The arrow represents the macroscopic net transfer of oxygen. c) LSV curves of LOBs with different thicknesses of the electrolyte layer.

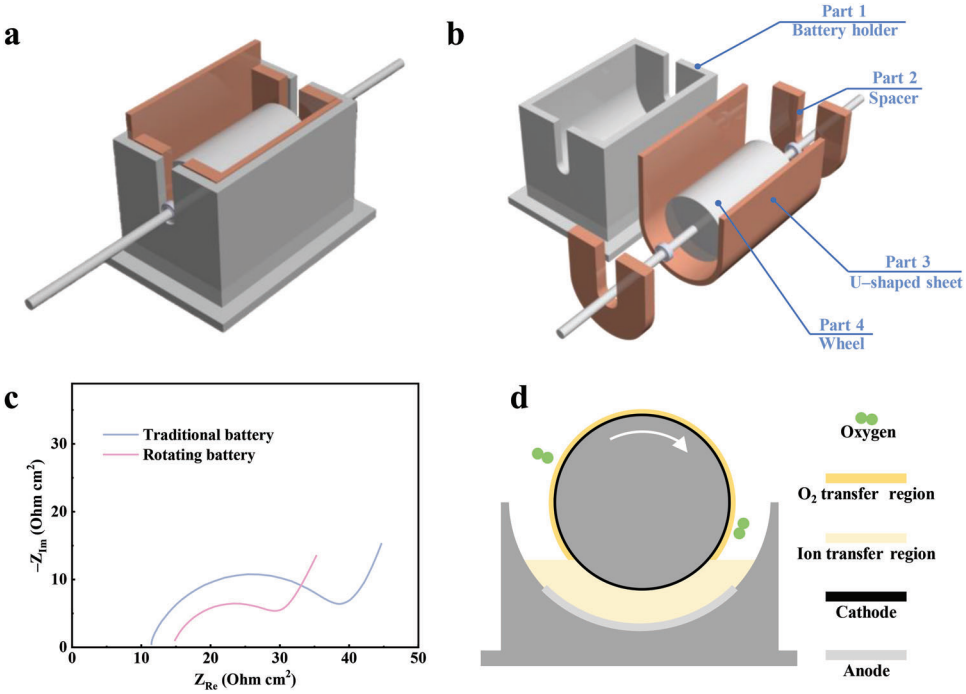

Figure 2. Schematic illustration of the LOB with a rotating cathode. a) Assembly and b) disassembly diagrams. c) Electrochemical impedance spectroscopy (EIS) of the traditional and rotating batteries (0 rpm). d) Schematic of the battery working principle.

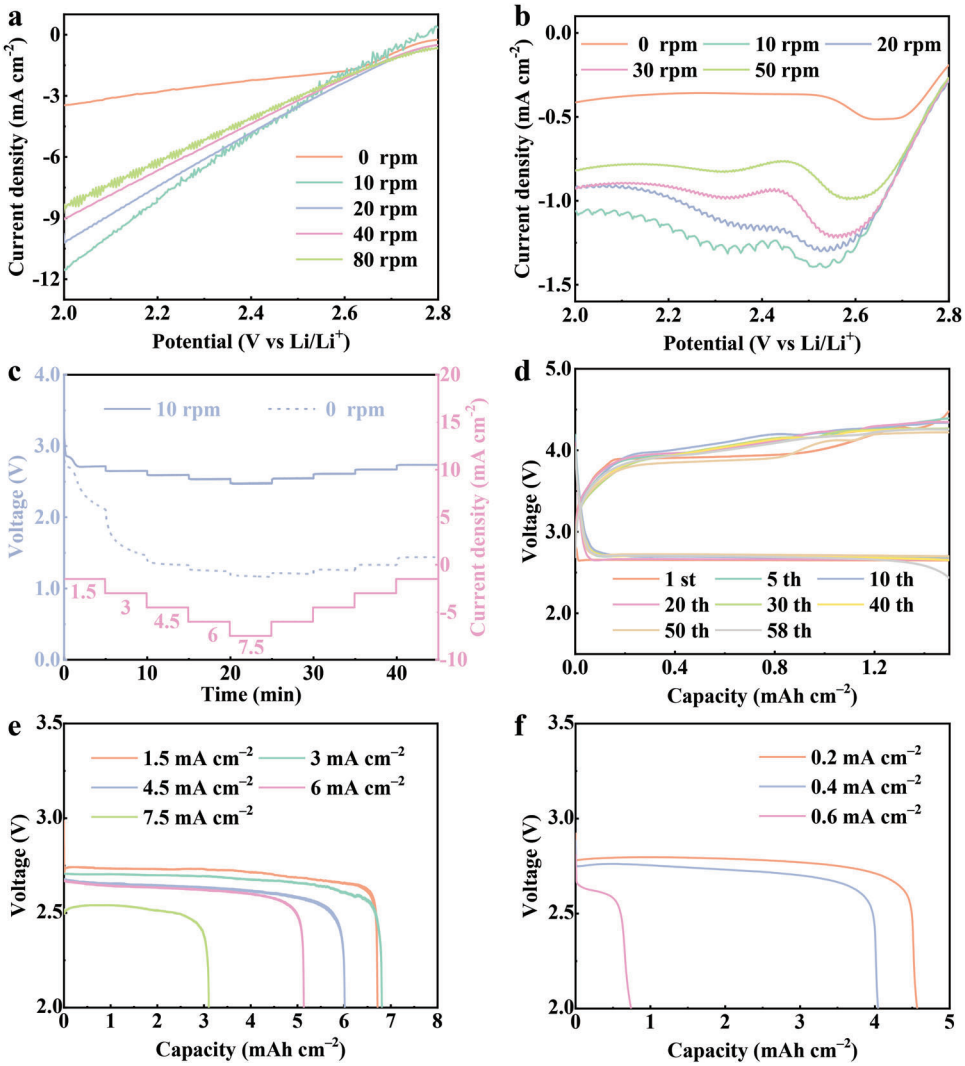

Figure 3. The electrochemical performance of rotating batteries. a) LSV curves of rotating batteries with pristine cathodes and b) cathodes that discharged to 2 V. c) Comparison of the discharge stability between batteries with the rotating and stationary electrodes. d) Cycling performance of the rotating battery at a current density of 2.5 mA cm^{-2}. Discharge capacities of the batteries at rotation speeds of e) 10 and f) 0 rpm.

anode is around 5 mm. Figure 2c is the electrochemical impedance spectroscopy (EIS) of the traditional coin battery and rotating battery. The bulk impedance of the two kinds of batteries is similar (11.4 Ohm cm^2 for the traditional battery and 14.8 Ohm cm^2 for the rotating battery), signifying that the design and manufacture of the rotating battery are reasonable.

When running the battery, only the portion of the cathode immersed in bulk electrolyte directly participates in the discharge process (Figure 2d). During discharge, the O_2 near the cathode within the bulk electrolyte is rapidly consumed. When the cathode rotates and moves away from the bulk electrolyte, most of the electrolyte on the cathode surface slides off, leaving a thin electrolyte layer, and the pores of the cathode are exposed to the O_2. Therefore, the O_2 can quickly go through the whole cathode and approach the electrode surface. Also, the O_2 dissolved in the electrolyte will return to the ion transfer region as the electrode continues to rotate. On the one hand, the electrolyte will refill the pores of the cathode, facilitating the transfer of Li^+. On the other hand, the rotating cathode would agitate the electrolyte, which is beneficial for thinning the diffusion layer of Li,$^{+}$[13] thereby ensuring a high Li^+ concentration near the cathode.

The motor that rotates the cathode is powered by an independent energy source which will consume some amount of energy. In fact, similar drive systems also exist in some mature batteries, like redox flow batteries, which require pumps to circulate the electrolytes. Fortunately, our device achieves satisfactory results at relatively low rotation speeds (10 rpm), where the energy consumed by rotating the cathode only accounts for about 10% of the energy provided by the battery (Figure S4, Supporting Information). It should be emphasized that this is merely a homemade and rudimentary setup, and we have reasons to believe that when it appears as a mature product, the power requirement for rotating the cathode will be much lower.

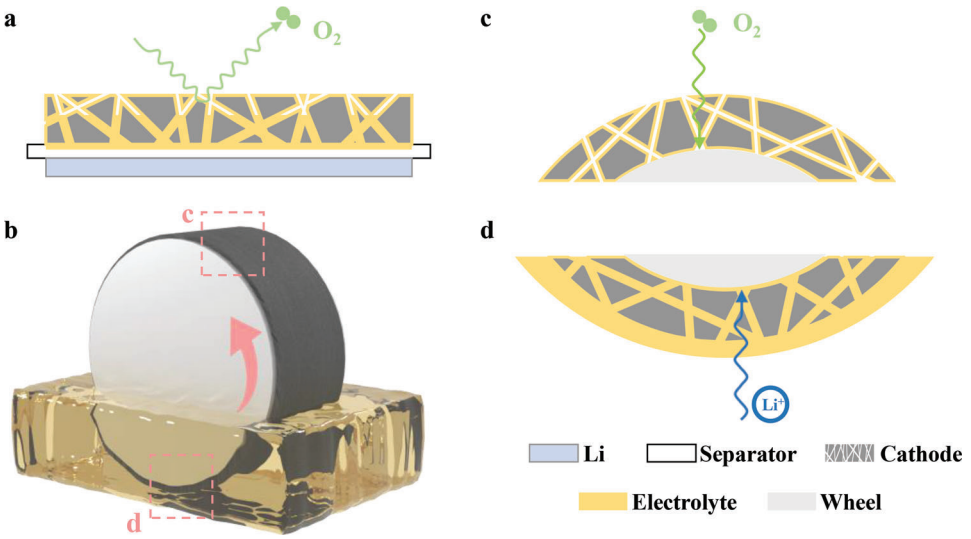

Figure 4. Schematic of the O_2 transfer pathways. a) Traditional batteries. b) Rotating batteries. (c,d) are enlarged views of the corresponding areas in (b).

2.3. Electrochemical Performance of the Rotating Battery

To demonstrate the enhanced mass transport enabled by the rotating cathode, the electrochemical performance of the battery was evaluated (**Figure 3**). Before discussing the electrochemical performance, we would like to illustrate the actual discharge area of the battery. As shown in Figure 1c, when there is only a small amount of electrolyte, the transfer of Li^+ will significantly limit the rate performance of LABs. Also, the amount of electrolyte on the upper half of the rotating cathode is less, which leads to the result that the electrode reaction almost entirely occurs in the cathode regions flooded in the bulk electrolyte (Figure S5, Supporting Information). Figure 3a depicts the LSV curves of the rotating battery at various rotation speeds. It is clear that the rotating cathode displays a much higher current response in the high polarization region than the stationary cathode. The rotation speed of the cathode for achieving the optimal rate performance is 10 rpm, which delivers a current three times higher than that at 0 rpm. However, further increasing the rotating speed will lead to a discernible decline in current. This is the consequence of changes in the thickness of the electrolyte with variations in cathode rotation speed. During the process of adjusting the rotation speed, the electrolyte on the cathode surface is relatively thin at low rotation speed. While the rotation speeds up, the electrolyte film tends to thicken. This phenomenon arises from the interaction between gravity and the inherent viscosity of the electrolyte. Under the influence of viscosity, a portion of the electrolyte disengages from the bulk electrolyte as the electrode rotates. Simultaneously, the electrolyte tends to flow back under the influence of gravity. At low speeds, gravity plays a prominent role, resulting in only a thin layer of electrolyte left on the cathode. As the rotation accelerates, the insufficient time for the electrolyte to flow down leads to its thickening. Additionally, the electrolyte could leave the electrode surface when further increasing the centrifugal force (rotation speed ≈500 rpm), leaving a thin electrolyte film again. However, due to the fact that the power consumed at high rotating speed by the motor exceeds the power that the LOBs can provide, further research has not been conducted.

In LOBs, the discharge products are lithium peroxide, an insulating substance. The accumulation of discharge products not only diminishes the active sites but also obstructs the transport pathway for both Li^+ and O_2. Therefore, the depth of discharge has a significant influence on the rate performance of LOBs. To demonstrate that the rotation of cathode is still beneficial for batteries at a fully discharged state, the batteries were discharged to 2 V and then retested the LSV curves at different rotating speeds (Figure 3b). Notably, compared to the battery without prior discharge, the current drops by almost an order of magnitude. Moreover, in the high polarization region, the *I*–*V* curves exhibit a distinct flattening trend, corresponding to the characteristic shape associated with mass-transfer control.[14] Despite the decreased current, the rotating cathode could still play an active role even if there are accumulated discharge products. Similarly, at the rotation speed of 10 rpm, the battery exhibits the highest rate performance, roughly twice the current of the stationary electrode. For LOBs, this implies that the sudden death of discharge will occur later, leading to a higher discharge capacity at the same current density.

Figure 3c compares the rate performance of batteries with rotation and stationary cathodes. When the cathode is in motion, the battery can return to its initial state after discharging at a maximum current density of 7.5 mA cm^{-2} for 5 min. However, with the stationary cathode, the battery rapidly deteriorates even under a low current density (1.5 mA cm^{-2}). Additionally, the LOBs with the rotation cathode could operate 58 cycles at a current density of 2.5 mA cm^{-2} with a limited capacity of 1.5 mAh cm^{-2} (Figure 3d), which is much better than the conventional batteries with a lifetime of only three cycles (Figure S6, Supporting Information). Figure 3e displays the discharge capacity curves of the batteries at different current densities. It is evident that the discharge capacities of the rotating batteries attenuate relatively slowly with the increase of current densities. Even at 7.5 mA cm^{-2}, the battery could still deliver a decent discharge capacity

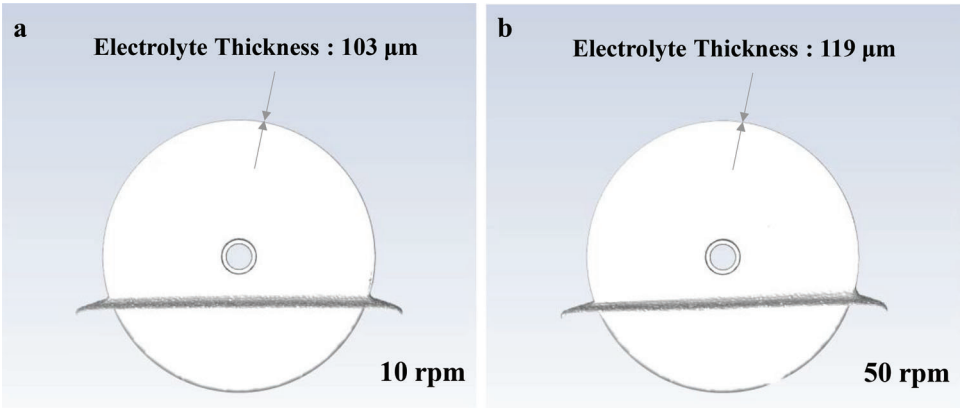

Figure 5. Simulation results of the electrolyte thickness at a) 10 and b) 50 rpm. In these two pictures, the system has reached a steady state, and the gray substance is the electrolyte.

(3.10 mAh cm^{-2}). Scanning electron microscope (SEM) images of the cathodes discharged to 2 V with different current densities are shown in Figure S7, Supporting Information. As the current density increases, the block-shaped discharge products gradually decrease, and eventually, all discharge products are film-like. The changed morphology of the discharge products may account for the better rate performance in the charge process.[15] Figure S8, Supporting Information, gives the X-ray diffraction (XRD) pattern of the discharged cathode at 7.5 mA cm^{-2}, which shows that the discharge product is lithium peroxide without other byproducts. For the battery with the stationary cathode, there is an obvious discharge capacity decrease only at 0.6 mA cm^{-2} (Figure 3f).

The enhanced performance of the rotating LOBs can be attributed to the changed mass transfer pathway induced by the rotating cathode. As depicted in **Figure 4a**, in a traditional battery, it is difficult for O_2 and Li^+ to go through the whole cathode, and simultaneously rapid Li^+ and O_2 transfer could only occur near the three-phase interface. However, for rotating batteries, the O_2 and Li^+ can rapidly go through the whole cathode in different areas of the rotating electrode (Figure 4c,d depicts the situation of O_2 transfer and Li^+ transfer, respectively). This unique mass transfer pathway effectively utilizes the reaction sites of the cathode, especially at high current densities, and accordingly leads to better rate performance and higher discharge capacity.

To illustrate the change in the thickness of the electrolyte layer on the rotating cathode, finite element analysis of the battery at different rotation speeds was carried out. The simulation was performed by ANSYS Fluent, utilizing the volume of fluid multiphase model, a model widely used for computing the gas-liquid-solid multiphase flow.[16] The contact angle (130 °, Figure S9, Supporting Information), viscosity (4.7 mPa s), and density (1.12 g cm^{-3}) of the electrolyte used in the calculations were obtained from the experimental measurements and are very close to the values reported in the literature.[17] **Figure 5a,b** show the thicknesses of the electrolyte at 10 and 50 rpm, respectively (the simulation results of other rotation speeds are shown in Figure S10, Supporting Information). The former is about 15% thinner than the latter, facilitating the O_2 access to the surface of the cathode. This result well supports our explanation of the improved rate performance brought by the rotating battery.

3. Conclusion

In summary, we have designed a new kind of battery with a rotating cathode that can periodically change the electrolyte layer thickness to achieve high-rate LOBs. The battery with the rotating cathode could discharge stably at 7.5 mA cm^{-2}, undergo 58 cycles at 2.5 mA cm^{-2}, and deliver a discharge capacity exceeding 6.8 mAh cm^{-2}. The performance improvement is attributed to the decoupling of the maximum transfer rate of Li^+ and O_2, which realizes the high-rate transfer of O_2 and Li^+ simultaneously. This new device opens promising avenues for high-rate LOBs and may also be useful for other electrochemical cells involving gas-liquid-solid triple-phase interfaces.

Supporting Information

Supporting Information is available from the Wiley Online Library or from the author.

Acknowledgements

Y.-L.L. and Y.Y. contributed equally to this work. This work was financially supported by the National Key R&D Program of China (2019YFA0705700), National Natural Science Foundation of China (U23A20575, U22A20437, 52171194, 52271140, 22209138), New Cornerstone Science Foundation through the XPLORER PRIZE, CAS Project for Young Scientists in Basic Research (YSBR-058), Guangdong Basic and Applied Basic Research Foundation (2021A1515110464), and National Natural Science Foundation of China Outstanding Youth Science Foundation of China (Overseas).

Conflict of Interest

The authors declare no conflict of interest.

Data Availability Statement

The data that support the findings of this study are available from the corresponding author upon reasonable request.

Keywords

high rate, Li–O_2 batteries, mass transfers, rotating cathodes

Received: March 3, 2024
Revised: April 11, 2024
Published online:

[1] a) Q. Qiu, J. Yuan, G. Li, Z. z. Pan, P. Yao, Y. Zhao, C. Zhang, Y. Li, *Adv. Mater. Technol.* **2023**, *8*, 2300743; b) Q. Qiu, Z.-Z. Pan, P. Yao, J. Yuan, C. Xia, Y. Zhao, Y. Li, *Chem. Eng. J.* **2023**, *452*, 139608; c) C. Xia, C. Kwok, L. Nazar, *Science* **2018**, *361*, 777; d) T. Liu, J. P. Vivek, E. W. Zhao, J. Lei, N. Garcia-Araez, C. P. Grey, *Chem. Rev.* **2020**, *120*, 6558; e) W. J. Kwak, Rosy, D. S., C. Xia, H. Kim, L. R. Johnson, P. G. Bruce, L. F. Nazar, Y. K. Sun, A. A. Frimer, M. Noked, S. A. Freunberger, D. Aurbach, *Chem. Rev.* **2020**, *120*, 6626; f) P. G. Bruce, S. A. Freunberger, L. J. Hardwick, J. M. Tarascon, *Nat. Mater.* **2011**, *11*, 19.

[2] a) N. Mahne, B. Schafzahl, C. Leypold, M. Leypold, S. Grumm, A. Leitgeb, G. A. Strohmeier, M. Wilkening, O. Fontaine, D. Kramer, C. Slugovc, S. M. Borisov, S. A. Freunberger, *Nat. Energy* **2017**, *2*, 17036; b) D. Wang, F. Zhang, P. He, H. Zhou, *Angew. Chem., Int. Ed.* **2019**, *58*, 2355.

[3] a) M. Mehta, V. Bevara, P. Andrei, *J. Power Sources* **2015**, *286*, 299; b) M. M. Thackeray, C. Wolverton, E. D. Isaacs, *Energy Environ. Sci.* **2012**, *5*, 7854; c) R. Padbury, X. Zhang, *J. Power Sources* **2011**, *196*, 4436.

[4] J.-G. Zhang, D. Wang, W. Xu, J. Xiao, R. E. Williford, *J. Power Sources* **2010**, *195*, 4332.

[5] a) F. S. Gittleson, R. E. Jones, D. K. Ward, M. E. Foster, *Energy Environ. Sci.* **2017**, *10*, 1167; b) J. Read, K. Mutolo, M. Ervin, W. Behl, J. Wolfenstine, A. Driedger, D. Foster, *J. Electrochem. Soc.* **2003**, *150*, A1351; c) J. Read, *J. Electrochem. Soc.* **2002**, *149*, A1190.

[6] F. Wang, X. Li, X. Hao, J. Tan, *ACS Appl. Energy Mater.* **2020**, *3*, 2258.

[7] a) A. Kraytsberg, Y. Ein-Eli, *Nano Energy* **2013**, *2*, 468; b) Y. Li, J. Wang, X. Li, D. Geng, R. Li, X. Sun, *Chem. Commun.* **2011**, *47*, 9438.

[8] C. Gaya, Y. Yin, A. Torayev, Y. Mammeri, A. A. Franco, *Electrochim. Acta* **2018**, *279*, 118.

[9] a) M. Chen, X. Jiang, H. Yang, P. K. Shen, *J. Mater. Chem. A* **2015**, *3*, 11874; b) Y. Cui, Z. Wen, X. Liang, Y. Lu, J. Jin, M. Wu, X. Wu, *Energy Environ. Sci.* **2012**, *5*, 7893.

[10] a) K. W. Beard, T. B. Reddy, *Linden's Handbook of Batteries*, McGraw-Hill Education, New York **2010**; b) C.-K. Park, Z. Zhang, Z. Xu, A. Kakirde, K. Kang, C. Chai, G. Au, L. Cristo, *J. Power Sources* **2007**, *165*, 892.

[11] a) A. Kube, F. Bienen, N. Wagner, K. A. Friedrich, *Adv. Mater. Interfaces* **2021**, *9*, 2101569; b) F. Wang, X. Li, *ACS Omega* **2018**, *3*, 6006; c) S. S. H. Zaidi, X. Li, *Adv. Energy Mater.* **2023**, *13*, 2300985.

[12] C. Qimeng, Z. Junxi, Y. Xujie, D. Nianwei, *J. Chin. Soc. Corros. Prot.* **2015**, *35*, 549.

[13] W. Wang, Q. Luo, B. Li, X. Wei, L. Li, Z. Yang, *Adv. Funct. Mater.* **2012**, *23*, 970.

[14] C. Prehal, A. Samojlov, M. Nachtnebel, L. Lovicar, M. Kriechbaum, H. Amenitsch, S. A. Freunberger, *Proc. Natl. Acad. Sci. U. S. A.* **2021**, *118*, 14.

[15] a) S.-M. Xu, X. Liang, X.-Y. Wu, S.-L. Zhao, J. Chen, K.-X. Wang, J.-S. Chen, *Nat. Commun.* **2019**, *10*, 5810; b) Q. Lv, Z. Zhu, Y. Ni, B. Wen, Z. Jiang, H. Fang, F. Li, *J. Am. Chem. Soc.* **2022**, *144*, 23239; c) Y. Li, R. Zhang, B. Chen, N. Wang, J. Sha, L. Ma, D. Zhao, E. Liu, S. Zhu, C. Shi, *Energy Storage Mater.* **2022**, *44*, 285.

[16] a) X. Sun, M. Sakai, *Chem. Eng. Sci.* **2015**, *134*, 531; b) Y. Xu, M. Liu, C. Tang, *Chem. Eng. J.* **2013**, *222*, 292.

[17] S. A. Markarian, M. Stockhausen, *Z. Phys. Chem.* **2000**, *214*, 139.